

Variational Monte Carlo calculations of ${}^3\text{H}$ and ${}^4\text{He}$ with a relativistic Hamiltonian

J. Carlson

Theoretical Division, Los Alamos National Laboratory, Los Alamos, New Mexico 87545

V. R. Pandharipande

Physics Department, University of Illinois, Urbana Campus, 1110 West Green Street, Urbana, Illinois 61801

R. Schiavilla

*Physics Division, Argonne National Laboratory, Argonne, Illinois 60439
and Istituto Nazionale di Fisica Nucleare, Sezione di Lecce, I-73100 Lecce, Italy*

(Received 22 June 1992)

The two-nucleon phase shifts and deuteron properties are fitted using relativistic, $(m^2 + p^2)^{1/2}$, kinetic-energy operators to obtain realistic models of \bar{v}_{ij} , the two-nucleon interaction in the frame in which the total momentum \mathbf{P}_{ij} of the interacting pair is zero. The relativistic Hamiltonian H_R contains the relativistic kinetic energy, \bar{v}_{ij} , and $\delta v_{ij}(\mathbf{P}_{ij})$ which describes the dependence of the interaction on the total momentum of the pair. The $\delta v_{ij}(\mathbf{P}_{ij})$ are obtained from the \bar{v}_{ij} using relativistic mechanics. The ground states of ${}^3\text{H}$ and ${}^4\text{He}$ are calculated using the H_R with the variational Monte Carlo method, and the results are compared with those obtained using the nonrelativistic H_{NR} . Results of calculations including the three-nucleon interaction are also reported. The relativistic effects reduce the binding energies of ${}^3\text{H}$ and ${}^4\text{He}$ by ~ 0.34 and 2.02 MeV, and they do not change the momentum distribution of the nucleons in these nuclei significantly.

PACS number(s): 21.45.+v, 27.10.+h, 21.60.-h

I. INTRODUCTION

The ground-state properties of nuclei, nuclear, and neutron star matter have often been studied with nonrelativistic quantum mechanics (NRQM) using the Hamiltonian

$$H_{NR} = \sum_i \frac{p_i^2}{2m} + \sum_{i < j} v_{ij} + \sum_{i < j < k} V_{ijk}. \quad (1.1)$$

NRQM calculations of nuclear binding energies are possible, with errors $< 10\%$, with the Brueckner-Bethe-Goldstone method, by going beyond two-hole-line terms [1,2] and by the more recently developed variational methods [3–5]. Exact calculations have also been carried out with the Green's-function Monte Carlo method [6,7] for nuclei having $A \leq 5$ and for the triton with the Faddeev method [8–10].

Realistic models of the two-nucleon interaction v_{ij} are obtained by fitting the N - N scattering data with NRQM. Several realistic models of v_{ij} give rather similar results; without any V_{ijk} , ${}^3\text{H}$ and ${}^4\text{He}$ are underbound and the equilibrium density of nuclear matter is too large. These difficulties can be mostly eliminated by using a three-nucleon interaction V_{ijk} that has an attractive, long-range, two-pion-exchange part $V_{ijk}^{2\pi}$ and a repulsive shorter-range part V_{ijk}^R . The strengths of $V_{ijk}^{2\pi}$ and V_{ijk}^R are obtained by fitting the binding energies of ${}^3\text{H}$ and ${}^4\text{He}$ and the saturation properties of nuclear matter [3,5]. Typically, the contribution of V_{ijk} is $\sim 3\%$ of that of v_{ij} in ${}^3\text{H}$ and ${}^4\text{He}$; however, because of a large cancellation between the kinetic and interaction energies, it is $\sim 15\%$ of the total binding energy.

The average value of p^2/m^2 in nuclei is ~ 0.05 , and thus it is possible that relativistic corrections to their binding energies are comparable with the contributions of V_{ijk} . The relativistic dynamics of interacting composite objects, such as nucleons, is nontrivial, and two different approaches have been used to study relativistic effects in nuclear binding energies.

In the first approach, the nucleons are described by Dirac spinors, which interact via exchange of observed mesons and "effective bosons". The theory is patterned after quantum electrodynamics and is elegantly relativistically covariant. Its mean-field limit [11,12] is rather simple, and it can describe nuclear ground states with an accuracy comparable to that of nonrelativistic mean-field theories based on Skyrme models. Lowest-order Dirac-Brueckner calculations [13–15] have also been carried out for nuclear matter with realistic interaction models. In this approach the antinucleon degrees of freedom, i.e., the lower components of the Dirac spinors, play an important role. Experimentally, however, there is no indication of a simple coupling of $N\bar{N}$ states to mesons or photons. In QCD also the coupling $N \rightarrow N + \text{meson}$ is not trivially related to the $N\bar{N} \rightarrow \text{mesons}$.

The other approach is based on the work of Bakamjian and Thomas [16] and Krajcik and Foldy [17] on relativistic dynamics. The Hamiltonian (1.1) is generalized to

$$H = \sum_i [(m^2 + p_i^2)^{1/2} - m] + \sum_{i < j} v(\mathbf{P}_{ij}) + \sum_{i < j < k} V_{ijk}(\mathbf{P}_{ijk}), \quad (1.2)$$

$$\mathbf{P}_{ij} = \mathbf{p}_i + \mathbf{p}_j, \quad (1.3)$$

$$\mathbf{P}_{ijk} = \mathbf{p}_i + \mathbf{p}_j + \mathbf{p}_k. \quad (1.4)$$

The interactions depend upon the total momentum of the interacting particles and may be written as

$$v_{ij}(\mathbf{P}_{ij}) = \bar{v}_{ij} + \delta v_{ij}(\mathbf{P}_{ij}), \quad (1.5)$$

$$V_{ijk}(\mathbf{P}_{ijk}) = \bar{V}_{ijk} + \delta V_{ijk}(\mathbf{P}_{ijk}), \quad (1.6)$$

where \bar{v}_{ij} (\bar{V}_{ijk}) is the interaction in the $\mathbf{P}_{ij}=0$ ($\mathbf{P}_{ijk}=0$) "rest frame" and $\delta v_{ij}(\mathbf{P}_{ij}=0)=0$ and $\delta V_{ijk}(\mathbf{P}_{ijk}=0)=0$. The rest-frame interactions \bar{v}_{ij} and \bar{V}_{ijk} can be determined by fitting the data, and relativistic covariance is used to obtain the momentum-dependent parts $\delta v_{ij}(\mathbf{P}_{ij})$ and $\delta V_{ijk}(\mathbf{P}_{ijk})$ from the \bar{v}_{ij} and \bar{V}_{ijk} . If the antinucleon degrees of freedom contribute to nuclear binding energies, then, in this approach, their contribution would have to be included in \bar{v}_{ij} and \bar{V}_{ijk} .

The relativistic corrections to the binding energies of nuclear matter [18] and the triton [19] have been estimated by Coester and co-workers using this approach, lowest-order Brueckner theory and the Faddeev method. It appears that the variational and Green's-function Monte Carlo methods can be effectively used to obtain accurate or exact solutions for the ground states of the relativistic Hamiltonian (1.2). In the present work, we report variational Monte Carlo (VMC) studies of the binding energies of ${}^3\text{H}$ and ${}^4\text{He}$ with the relativistic Hamiltonian.

In Sec. II we describe a realistic model of \bar{v}_{ij} obtained by fitting the N - N phase shifts and deuteron properties with the relativistic two-body Hamiltonian in the $\mathbf{P}_{12}=0$ frame:

$$H_R = 2[(m^2 + p^2)^{1/2} - m] + \bar{v}_{12}, \quad (1.7)$$

$$\mathbf{P}_1 = -\mathbf{P}_2 = \mathbf{P}. \quad (1.8)$$

Here \bar{v}_{ij} is assumed to have the form of the Urbana [20] v_{14} interaction. It has a one-pion-exchange long-range part and a soft repulsive core of finite height.

Variational Monte Carlo calculations of ${}^3\text{H}$ and ${}^4\text{He}$, with the semirelativistic Hamiltonian

$$H_{\text{SR}} \equiv \sum_i [(m^2 + p_i^2)^{1/2} - m] + \sum_{i < j} \bar{v}_{ij} + \sum_{i < j < k} \bar{V}_{ijk} \quad (1.9)$$

are reported in Sec. III. The momentum distribution of nucleons in ${}^3\text{H}$ is also discussed in this section. Because of the assumed soft-core nature of \bar{v}_{ij} , the maximum momentum of nucleons is $\sim m$, suggesting that the probability of P_{ij} being greater than m is negligibly small.

A pedagogical discussion of $\delta v_{ij}(\mathbf{P}_{ij})$ based on classical relativistic mechanics is given in Sec. IV. Note that the relativistic Hamiltonian (1.2) is given by

$$H_R \equiv H_{\text{SR}} + \sum_{i < j} \delta v_{ij}(\mathbf{P}_{ij}) + \sum_{i < j < k} \delta V_{ijk}(\mathbf{P}_{ijk}). \quad (1.10)$$

Here $\delta v_{ij}(\mathbf{P}_{ij})$ is expanded in powers of $P_{ij}^2/4m^2$, and only the leading term of order $P_{ij}^2/4m^2$ is kept. Its contribution is calculated perturbatively; it is very small, $\sim 1\%$ of that of \bar{v}_{ij} , and that of $\delta V_{ijk}(\mathbf{P}_{ijk})$ is neglected. The results are discussed and compared with those of Ref. [19] in Sec. V.

II. REALISTIC MODEL OF \bar{v}_{ij}

The two-nucleon interaction \bar{v}_{ij} is taken as a sum of 14 operator components:

$$\bar{v}_{ij} = \sum_{p=1}^{14} [\bar{v}_{\pi}^p(r_{ij}) + \bar{v}_I^p(r_{ij}) + \bar{v}_S^p(r_{ij})] O_{ij}^p, \quad (2.1)$$

where the operators O_{ij}^p are

$$O_{ij}^{p=2n-1} = 1, \quad \sigma_i \cdot \sigma_j, \quad S_{ij}, \quad \mathbf{L} \cdot \mathbf{S}, \quad L^2, \quad L^2 \sigma_i \cdot \sigma_j, \quad (\mathbf{L} \cdot \mathbf{S})^2, \quad (2.2)$$

$$O_{ij}^{p=2n} = O_{ij}^{p=2n-1} \tau_i \cdot \tau_j, \quad (2.3)$$

and $n = 1, \dots, 7$. Here S_{ij} is the tensor operator, \mathbf{L} the relative angular momentum, and \mathbf{S} the total spin of the pair. It is convenient to use the letters $c, \tau, \sigma, \sigma\tau, t, t\tau, b, b\tau, q, q\tau, q\sigma, q\sigma\tau, bb$, and $bb\tau$ in referring to the terms $p = 1-14$, respectively. The occurrence of the first eight operators in Eq. (2.1) is uniquely determined by the two-nucleon singlet and triplet S - and P -wave phase shifts. The L^2 -dependent terms differentiate S and D waves, and P and F waves, while the $(\mathbf{L} \cdot \mathbf{S})^2$ components provide a third independent way (in addition to the S_{ij} and $\mathbf{L} \cdot \mathbf{S}$ operators) for splitting triplet states with different J values, such as ${}^3D_{1,2,3}$ states. It should be emphasized that the last six operators are not uniquely identified. The operator structure of \bar{v} is identical to that of the Urbana [20] and Argonne [21] potential models. However, in the Paris [22] potential model, the last six operators are replaced by four terms quadratic in \mathbf{p} (\mathbf{p} is the relative momentum of the pair) and two terms quadratic in \mathbf{L} .

The 14 operators in Eq. (2.1) provide sufficient flexibility to characterize the 14 singlet and triplet S -, P -, D -, and F -wave phase shifts. The potential includes a long-range, one-pion-exchange (OPE) part $\bar{v}_{\pi}^p(r)$, which is nonzero only for $p = \sigma\tau$ and $t\tau$. Here $\bar{v}_{\pi}^{p=\sigma\tau}$ and $\bar{v}_{\pi}^{p=t\tau}$ are the usual Yukawa and tensor functions modified by smooth Gaussian cutoffs which make them vanish at $r = 0$,

$$\begin{aligned} \bar{v}_{\pi}^{\sigma\tau}(r) &= \left[\frac{\mu}{3} \frac{f_{\pi}^2}{4\pi} \right] \frac{e^{-\mu r}}{\mu r} (1 - e^{-cr^2}) \\ &\equiv (3.635 \text{ MeV}) Y_{\pi}(r), \end{aligned} \quad (2.4)$$

$$\begin{aligned} \bar{v}_{\pi}^{t\tau}(r) &= \left[\frac{\mu}{3} \frac{f_{\pi}^2}{4\pi} \right] \frac{e^{-\mu r}}{\mu r} \left[1 + \frac{3}{\mu r} + \frac{3}{\mu^2 r^2} \right] (1 - e^{-cr^2})^2 \\ &\equiv (3.635 \text{ MeV}) T_{\pi}(r). \end{aligned} \quad (2.5)$$

The Gaussian cutoff of $\bar{v}_{\pi}^{t\tau}$ should simulate the effects due to ρ -meson-exchange interactions [23]. The parameter c is taken as 2 fm^{-2} , while the coefficients in brackets are calculated using $f_{\pi}^2/4\pi = 0.079$ and $\mu = 0.69953 \text{ fm}^{-1}$, with $\hbar c = 197.327 \text{ MeV fm}$. The intermediate range part $\bar{v}_I^p(r)$ is assumed to come mainly from two-pion-exchange processes, such as those associated with the intermediate excitation of a Δ isobar. As these have predominantly tensor character, we have taken

$$\bar{v}_I^p(r) = I^p T_{\pi}^2(r). \quad (2.6)$$

TABLE I. Potential strengths in singlet states (MeV) for the \bar{v}_{14} model.

p	I_{10}^p	$S_{1,10}^p$	$S_{2,10}^p$	I_{60}^p	$S_{1,00}^p$	$S_{2,00}^p$
c	-8.663	3042.2	90.21	-8.196	5515.	319.1
q	0.08033	78.01	-32.12	0.3926	-93.48	-1221.

Finally, the short-range part is parametrized as a sum of two Woods-Saxon functions,

$$\bar{v}_S^p(r) = \frac{S_1^p}{1 + e^{(r-R_1)/a_1}} + \frac{S_2^p}{1 + e^{(r-R_2)/a_2}} \equiv S_1^p W_1(r) + S_2^p W_2(r). \quad (2.7)$$

The values used for R_1 (R_2) and a_1 (a_2) are 0.5 (0.36) and 0.2 (0.16) fm, respectively. These values as well as that for c are the same as those used in the Urbana and Argonne potentials. The parameters I^p , S_1^p , and S_2^p are determined by fitting the np phase shifts up to energies of 400 MeV in the laboratory and deuteron properties with the relativistic two-body Hamiltonian (1.7). However, rather than fitting the phase shifts obtained from the analysis of nucleon-nucleon scattering data, we have chosen to fit the phase shifts calculated with the nonrelativistic Argonne v_{14} interaction and the nonrelativistic kinetic energy.

We have attempted to make the present \bar{v}_{14} phase-shift equivalent to the Argonne $v_{14,NR}$, since our main interest is to study the differences between the nuclear properties predicted by nonrelativistic calculations with the Argonne $v_{14,NR}$ and the present calculations using a relativistic

Hamiltonian based upon \bar{v}_{14} .

The potential operators in channels with isospin T and spin S are denoted by \bar{v}_{TS} . In the $S=0$ singlet channels and $S=1$ triplet channels, we have

$$\bar{v}_{T0} = \bar{v}_{T0}^c + \bar{v}_{T0}^q L^2, \quad (2.8)$$

$$\bar{v}_{T1} = \bar{v}_{T1}^c + \bar{v}_{T1}^i S_{ij} + \bar{v}_{T1}^b \mathbf{L} \cdot \mathbf{S} + \bar{v}_{T1}^q L^2 + \bar{v}_{T1}^{bb} (\mathbf{L} \cdot \mathbf{S})^2, \quad (2.9)$$

and

$$\bar{v}_{TS}^c = \bar{v}_{\pi,TS}^c(r) + I_{TS}^c T_\pi^2(r) + S_{1,TS}^c W_1(r) + S_{2,TS}^c W_2(r). \quad (2.10)$$

The other \bar{v}_{TS}^p are also similarly expressed; however, the tensor \bar{v}_{T1}^i does not have short-range terms, and only the \bar{v}_{TS}^c and \bar{v}_{T1}^i have pion-exchange terms.

The strengths I_{TS}^p , $S_{1,TS}^p$, and $S_{2,TS}^p$ are determined from the fits, and their values are listed in Tables I and II. The values for I^p , S_1^p , and S_2^p used in Eqs. (2.6) and (2.7) are easily obtained from these. Standard momentum-space techniques are used to solve for the K matrix in the JTS channel [24]:

$$K_{L',L}^{JTS}(p',p) = \bar{v}_{L',L}^{JTS}(p',p) + \frac{2}{\pi} \int_0^\infty dk k^2 \bar{v}_{L',L}^{JTS}(p',k) \frac{\mathcal{P}}{2(p^2 + m^2)^{1/2} - 2(k^2 + m^2)^{1/2}} K_{L',L}^{JTS}(k,p), \quad (2.11)$$

where \mathcal{P} denotes principal value,

$$\bar{v}_{L',L}^{JTS}(p',p) = \int_0^\infty dr r^2 j_{L'}(p'r) \bar{v}_{L',L}^{JTS}(r) j_L(pr) \quad (2.12)$$

and

$$\bar{v}_{L',L}^{JTS}(r) = \int d\Omega y_{L'SJ}^{M_J^\dagger} \bar{v}_{TS} y_{LSJ}^{M_J}. \quad (2.13)$$

Here the $j_L(x)$ are spherical Bessel functions and $y_{LSJ}^{m_J}$ are spin-angle tensors. The K matrix is real and symmetric, and is related to the on-shell S matrix via

$$ip(p^2 + m^2)^{1/2} K^{JTS}(pp) = [1 - S^{JTS}(pp)] [1 + S^{JTS}(pp)]^{-1}, \quad (2.14)$$

in obvious matrix notation. The momentum p is given by $p = \sqrt{mT_{\text{lab}}}/2$, T_{lab} being the kinetic energy in the laboratory (this latter relation is identical to that in the nonrelativistic case). From the S matrix, the phase shifts are easily obtained. The integral equation (2.11) is discretized, and the resulting system of linear equations is solved by direct numerical inversion. Care must be taken to accurately calculate the Bessel transforms in Eq. (2.12). The principal-value integration in Eq. (2.11) is eliminated by a standard subtraction technique [24]. A similar method can be used to calculate the deuteron momentum-space wave functions $u_L(p)$, $L=0,2$. They satisfy the homogeneous integral equation

TABLE II. Potential strengths in triplet states (MeV) for the \bar{v}_{14} model.

p	I_{61}^p	$S_{1,01}^p$	$S_{2,01}^p$	I_{11}^p	$S_{1,11}^p$	$S_{2,11}^p$
c	-6.682	2882.1	-866.6	-4.452	2402.0	-1846.0
t	0.6440	0	0	-0.1409	0	0
b	0.1042	37.86	14.58	0.2318	-52.22	-3145.0
q	0.7110	175.4	-527.1	-0.2038	-129.9	1148.0
bb	-0.9252	75.26	55.59	-0.002418	116.9	846.9

$$u_L(p) = \frac{1}{2m + E_d - 2(p^2 + m^2)^{1/2}} \frac{2}{\pi} \times \int_0^\infty dk k^2 \bar{v}_{L,L}^{101}(pk) u_L(k), \quad (2.15)$$

and E_d is the deuteron eigenvalue.

As stated above, \bar{v}_{14} has the same operator structure as the Urbana and Argonne interactions, and is almost phase-shift equivalent to the Argonne $v_{14,\text{NR}}$. There are three differences between the \bar{v}_{14} and the Argonne $v_{14,\text{NR}}$: First, the value for f_π^2 in \bar{v}_{14} is $\approx 2\%$ smaller than that of $v_{14,\text{NR}}$; second, as in the Urbana potential, we do not allow for short-range tensor components in \bar{v}_{14} , namely, $S_{1,T}^i = S_{2,T}^i = 0$ for $T=0$ and 1; third, the short-range part is parametrized as a sum of Woods-Saxon functions rather than a single one as in the Argonne $v_{14,\text{NR}}$.

The $v_{14,\text{NR}}$ phases in singlet 1S_0 , 1P_1 , and 1D_2 states are almost exactly reproduced by the present \bar{v}_{14} , as can be seen in Figs. 1–3. The central potentials \bar{v}_{10}^c and \bar{v}_{00}^c in the $S=0$ states are compared with their nonrelativistic counterparts in Fig. 4. The relativistic (R) and NR $v_{T,S=0}^c$ are similar, though the R potentials have slightly larger repulsive cores, and the \bar{v}_{10}^c is also a little less attractive than $v_{10,\text{NR}}^c$. The wave functions can be bent more easily when the relativistic kinetic-energy operator is used in place of the nonrelativistic. Hence \bar{v}_{10}^c has to be more repulsive and less attractive than $v_{10,\text{NR}}^c$ to maintain phase equivalence.

It is more difficult to compare the present \bar{v}_{14} with the Argonne $v_{14,\text{NR}}$ in the $S=1$ triplet states because of differences in the tensor forces. The phase shifts given by these two models and the Urbana $v_{14,\text{NR}}$ in 3S_1 , 3P_1 , and 3D_1 states are compared in Figs. 5–14. The $S=1$, \bar{v} and Ar-

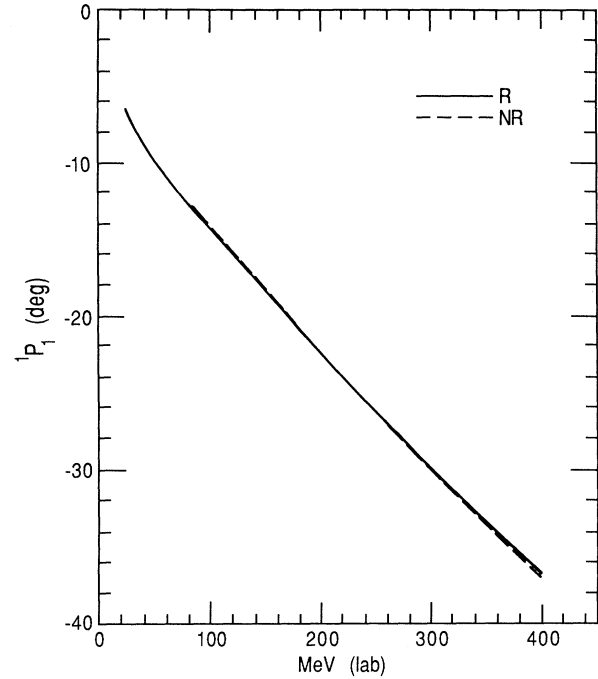


FIG. 2. 1P_1 phase shifts in the notation of Fig. 1.

gonne $v_{14,\text{NR}}$ forces are not as phase equivalent as the $S=0$ forces. Typically, the differences between the \bar{v} and Argonne $v_{14,\text{NR}}$ phase shifts are smaller than those between the Urbana and Argonne NR potentials. The binding energies obtained with the Urbana and Argonne NR models for ${}^3\text{H}$ and ${}^4\text{He}$ are not very different, and hence

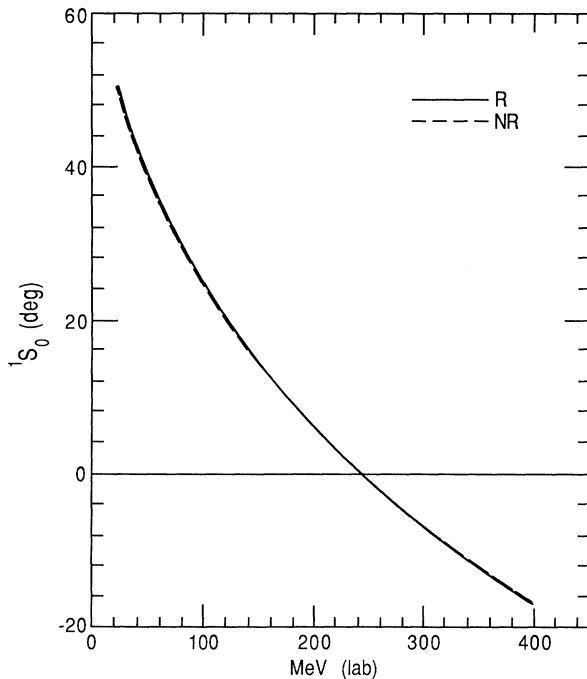


FIG. 1. 1S_0 phase shifts obtained with the relativistic \bar{v} (solid line) and Argonne $v_{14,\text{NR}}$ (dashed line) interactions.

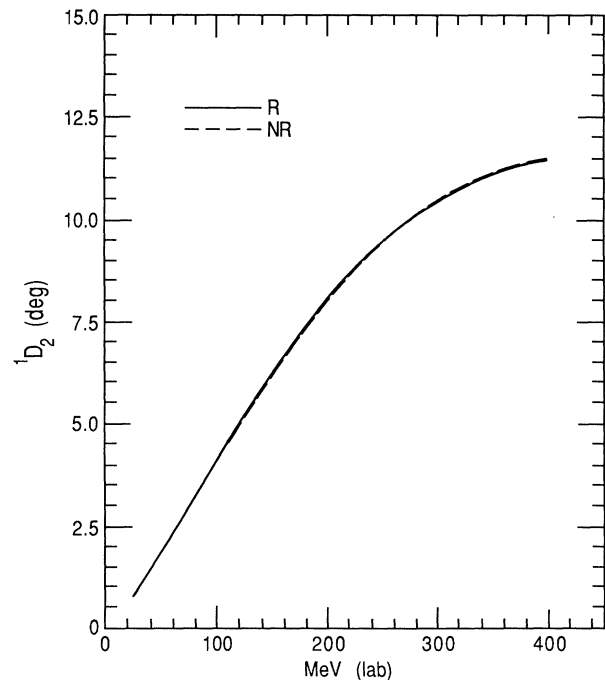


FIG. 3. 1D_2 phase shifts in the notation of Fig. 1.

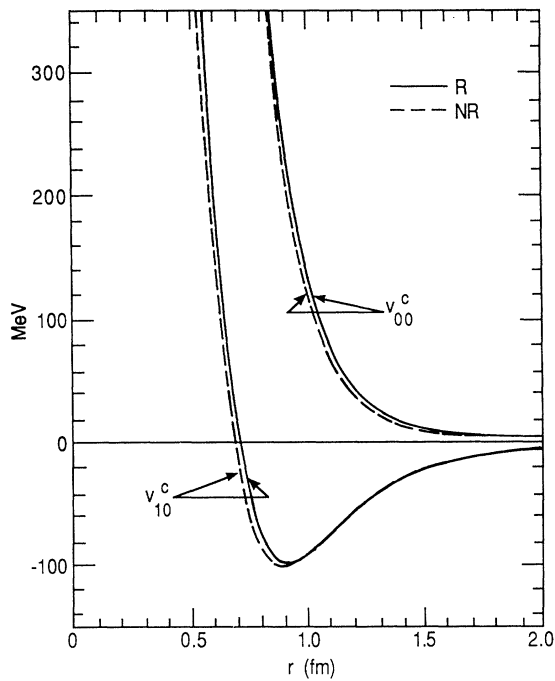


FIG. 4. Central potential in $TS = 10$ and 00 states in the \bar{v} (solid lines) and Argonne $v_{14,NR}$ (dashed lines) models.

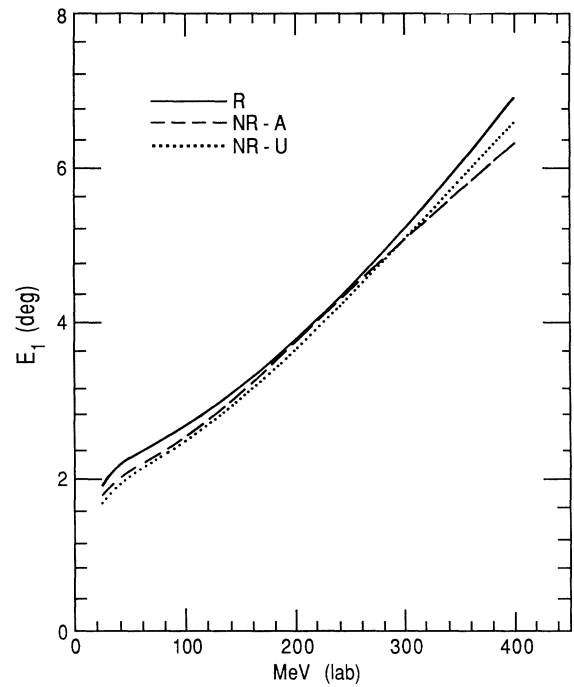


FIG. 6. E_1 in the notation of Fig. 5.

we can hope that the magnitude of the differences between the R and NR phase shifts is not very significant. Note that the phases in the 3S_1 - 3D_1 states, which are particularly important in ${}^3\text{H}$ and ${}^4\text{He}$, are rather similar for the R and Argonne $v_{14,NR}$ models.

The central, tensor, and spin-orbit potentials in the

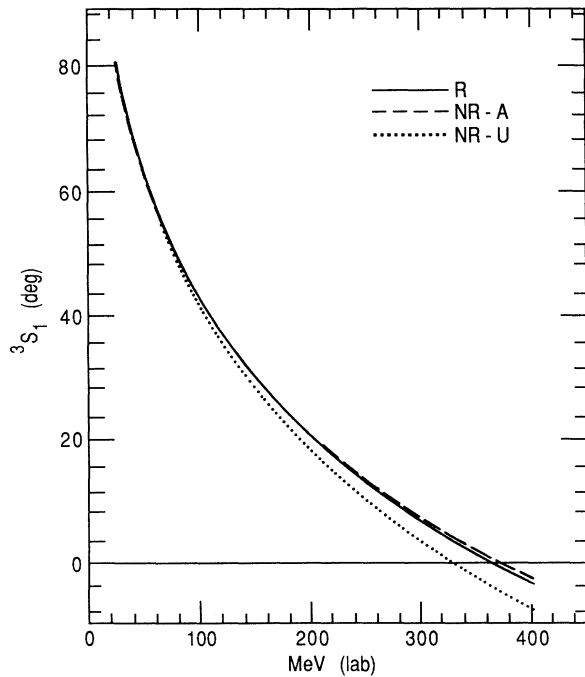


FIG. 5. 3S_1 phase shifts obtained with the relativistic \bar{v} (solid line), Argonne $v_{14,NR}$ (dashed line), and Urbana $v_{14,NR}$ (dotted line) interactions.

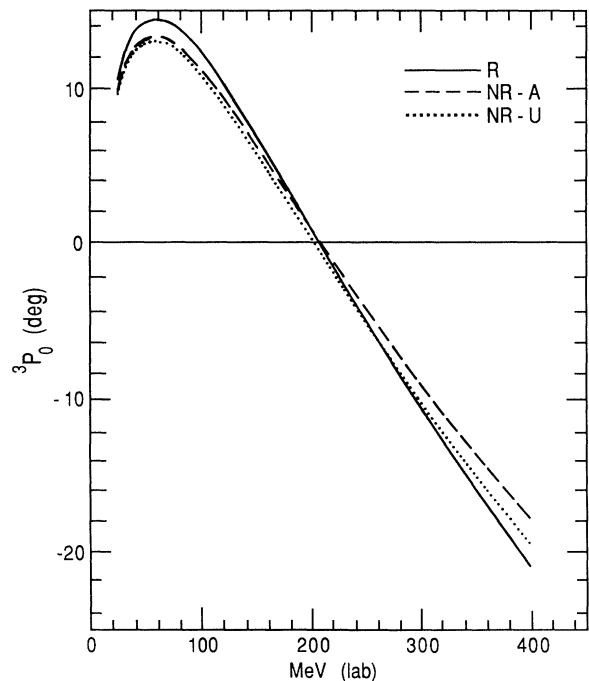
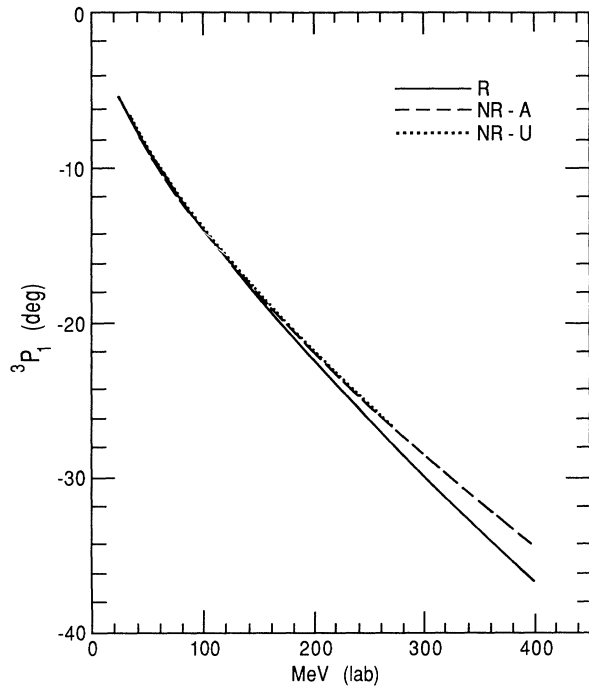
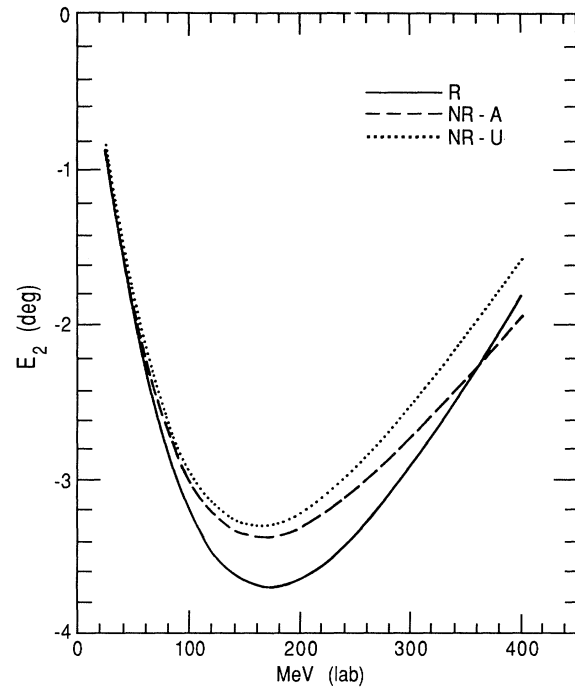
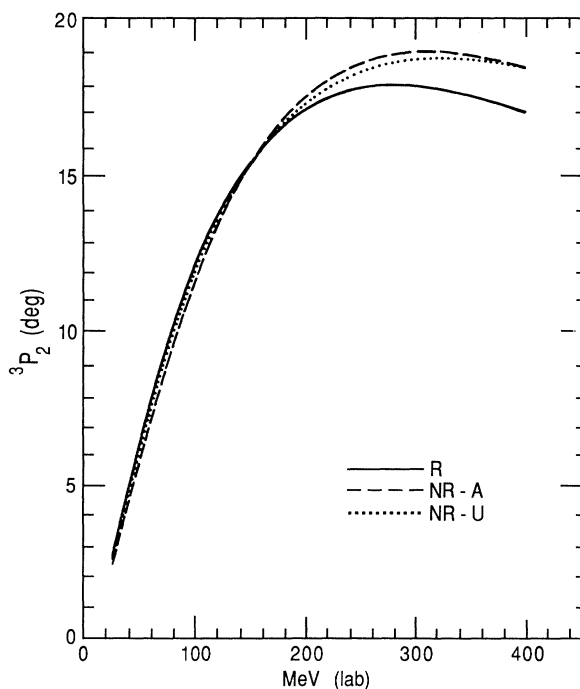
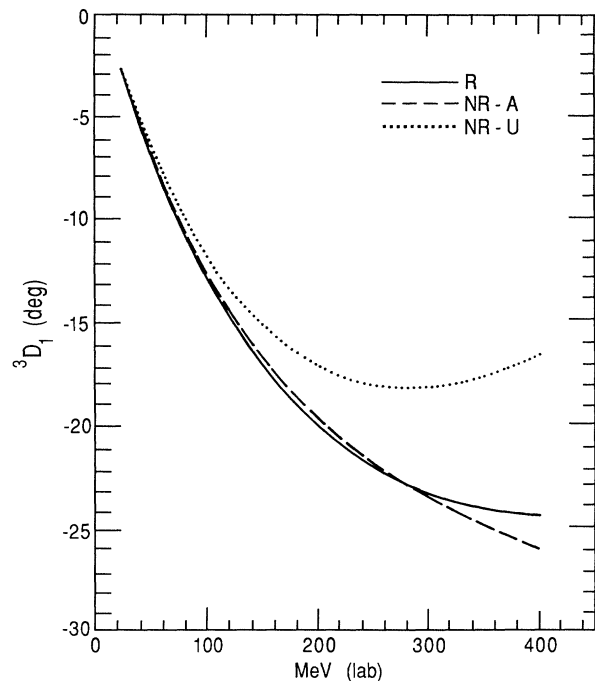


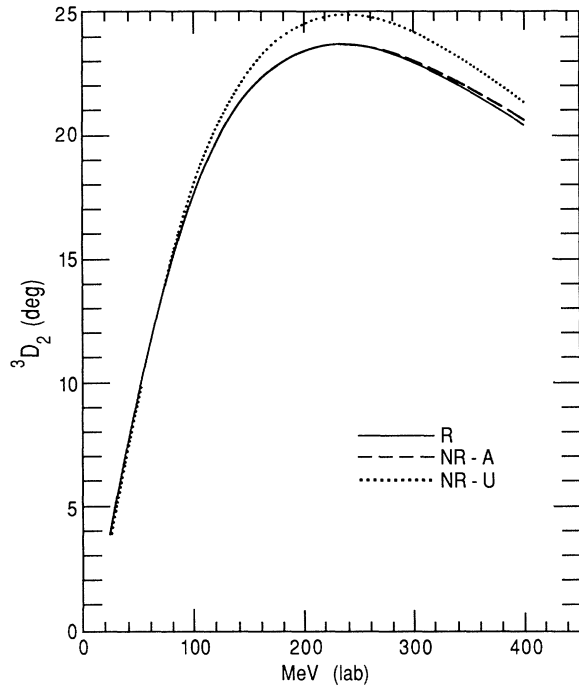
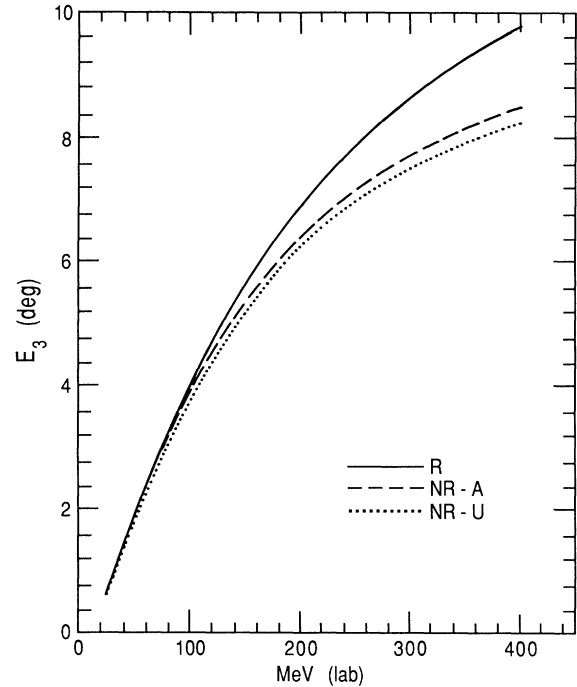
FIG. 7. 3P_0 phase shifts in the notation of Fig. 5.

FIG. 8. 3P_1 phase shifts in the notation of Fig. 5.FIG. 10. E_2 in the notation of Fig. 5.

$S=1$ states are compared in Figs. 15–17. Here \bar{v}_{01}^c is more attractive than the Argonne $v_{01,\text{NR}}^c$, presumably because the tensor potential is weaker in the R interaction; \bar{v}_0^b is positive as in the Urbana $v_{14,\text{NR}}$, while that in the Argonne $v_{14,\text{NR}}$ is negative. This difference is also due to that in the behavior of v_0' at small r .

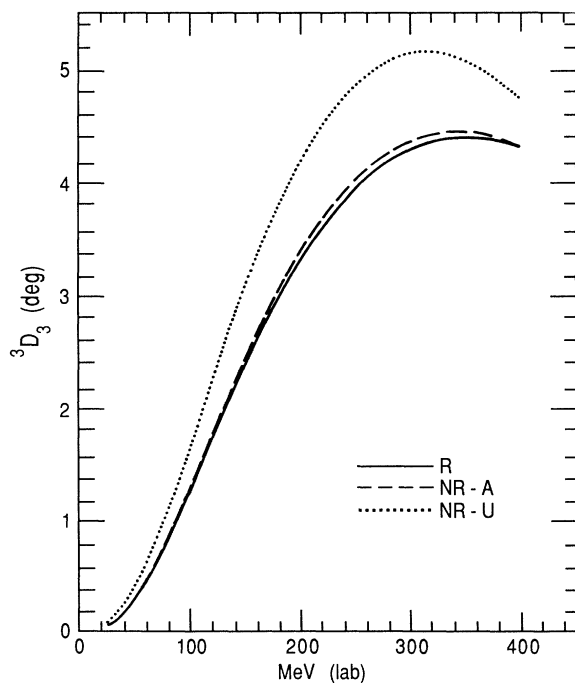
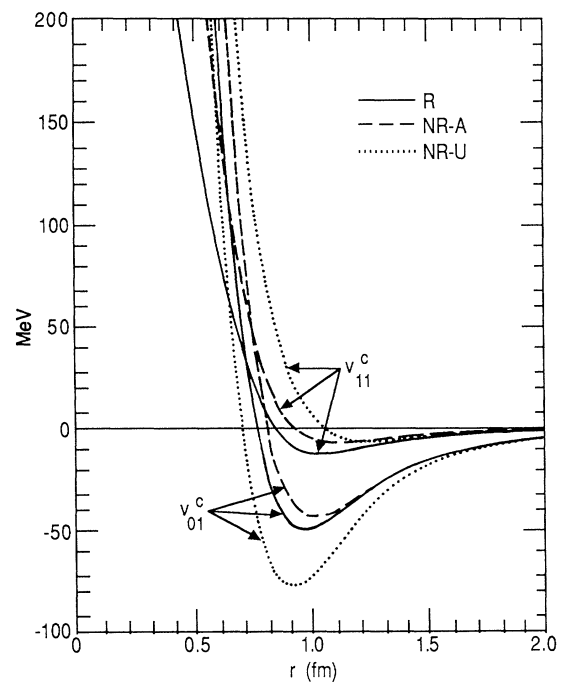
The deuteron S - and D -wave functions are shown in Fig. 18, and the momentum distributions are compared in Fig. 19. The R deuteron $n(k)$ has a minimum at $k \approx 6.8 \text{ fm}^{-1}$. The NR Urbana $n(k)$ has a structure at this value of k which gets developed into a minimum in the R model. It is due to a diffraction minimum in the

FIG. 9. 3P_2 phase shifts in the notation of Fig. 5.FIG. 11. 3D_1 phase shifts in the notation of Fig. 5.

FIG. 12. 3D_2 phase shifts in the notation of Fig. 5.FIG. 14. E_3 in the notation of Fig. 5.

Fourier transform of the D -state wave function, and it may be possible to eliminate it or move its position by changing the tensor force at small r .

The observed deuteron properties and the singlet and triplet scattering lengths and effective ranges are listed in Table III. These show the equivalence of the R and NR

FIG. 13. 3D_3 phase shifts in the notation of Fig. 5.FIG. 15. Central potentials in $TS=01$ and 11 states in the \bar{u} (solid line), Argonne $v_{14,NR}$ (dashed line), and Urbana $v_{14,NR}$ (dotted line) models.

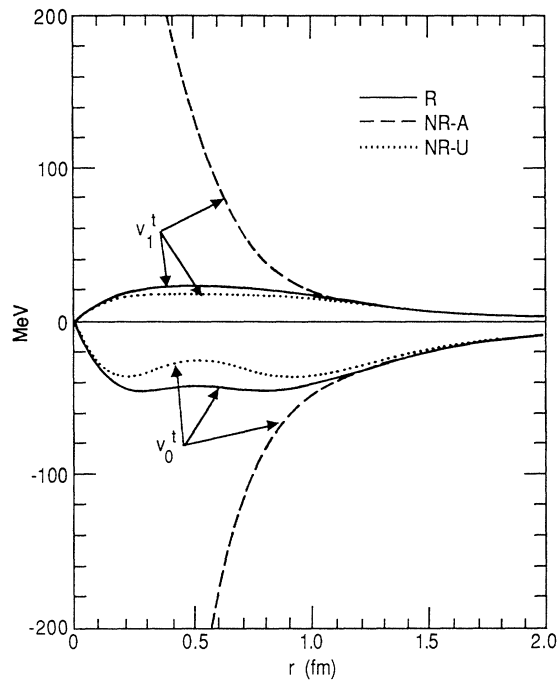


FIG. 16. Tensor potentials in $T=0$ and 1 states in the notation of Fig. 15.

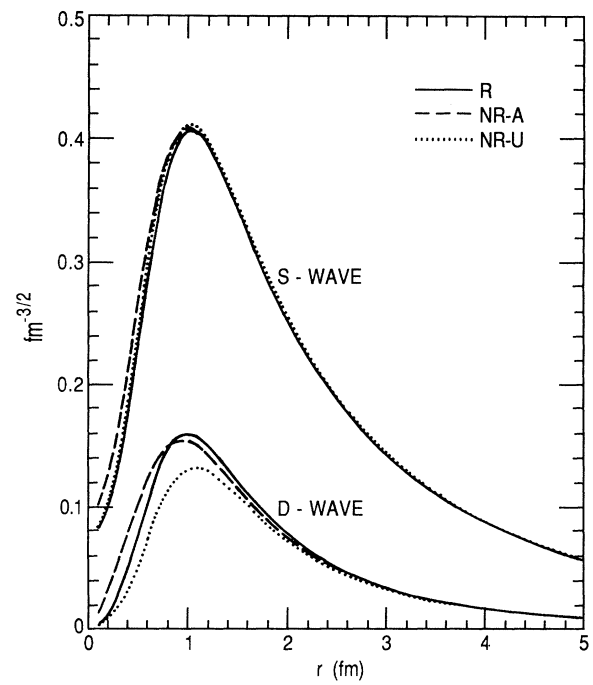


FIG. 18. Deuteron S- and D-wave functions in the notation of Fig. 15.

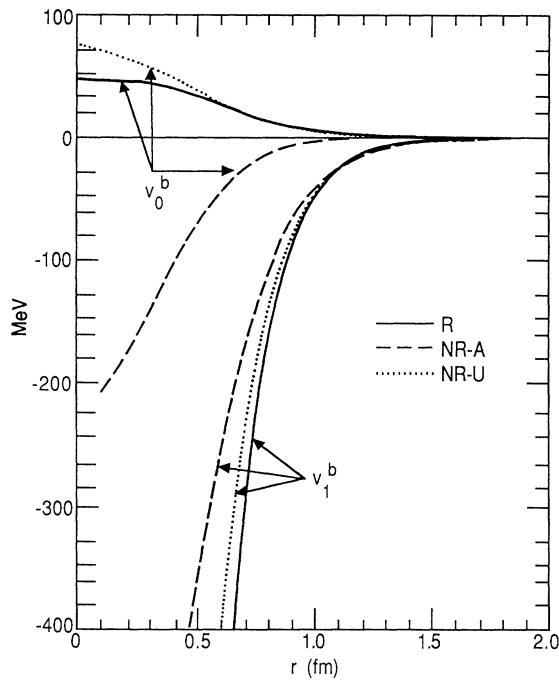


FIG. 17. Spin-orbit potentials in $T=0$ and 1 states in the notation of Fig. 15.

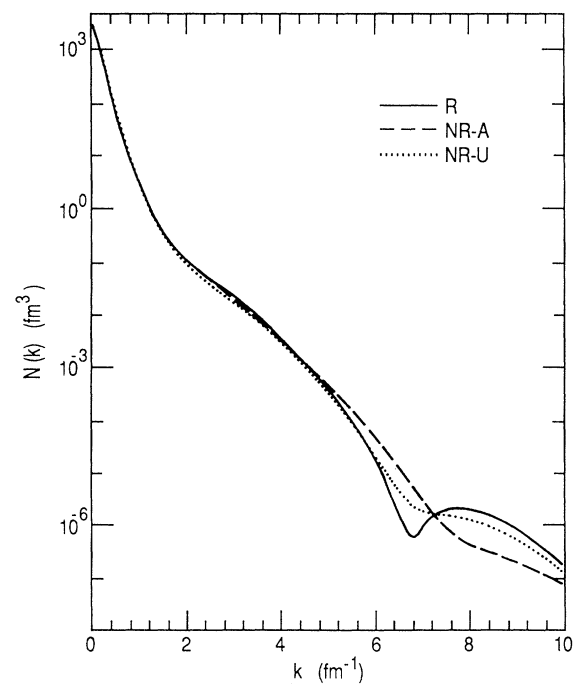


FIG. 19. Momentum distribution of the nucleons in deuteron in the notation of Fig. 15.

TABLE III. Deuteron properties and effective range parameters.

	\bar{v}_{14}	$v_{14, \text{NR}}$
E_d (MeV)	-2.2249	-2.2250
Q_d (fm ²)	0.289	0.286
η_d	0.0265	0.0266
${}^3a_{np}$ (fm)	5.44	5.45
${}^3r_{np}$ (fm)	1.73	1.80
${}^1a_{np}$ (fm)	-23.67	-23.67
${}^1r_{np}$ (fm)	2.81	2.77

models at low energies. The D state accounts for 6.43% and 6.08% of the deuteron wave function in the R and NR Argonne models, respectively.

III. VARIATIONAL MONTE CARLO CALCULATIONS

Variational Monte Carlo (MC) calculations with H_{SR} [Eq. (1.9)] are analogous to those carried out with NRQM [3,6]. The variational wave functions are of the form

$$\Psi_v = \left[S \prod_{i < j} F_{ij} \right] |\Phi\rangle, \quad (3.1)$$

having a symmetrized product of correlation operators F_{ij} operating on an antisymmetric, uncorrelated wave function $|\Phi\rangle$. The expectation values of \bar{v}_{ij} and \bar{V}_{ijk} are calculated as in the NR calculations. The main difference between H_{SR} and H_{NR} is in the kinetic-energy operator.

Contrary to naive expectations, it is rather simple to evaluate the expectation value of the square-root kinetic-energy operator in coordinate space with the MC method. The required expressions are obtained from the identity

$$\langle \Psi_l | (p_i^2 + m^2)^{1/2} - m | \Psi_r \rangle = \lim_{\Delta\tau \rightarrow 0} \frac{1}{\Delta\tau} \langle \Psi_l | (1 - \exp\{-\Delta\tau[(p_i^2 + m^2)^{1/2} - m]\}) | \Psi_r \rangle. \quad (3.2)$$

The above expectation value is calculated using the free-particle imaginary-time propagator $G(\mathbf{r})$:

$$\langle \Psi_l | \exp[-\Delta\tau(p_i^2 + m^2)^{1/2}] | \Psi_r \rangle = \int d\mathbf{R} \int d\mathbf{r}'_i \Psi_l^\dagger(\mathbf{R} + \mathbf{r}'_i) G(\mathbf{r}'_i) \Psi_r(\mathbf{R}), \quad (3.3)$$

where \mathbf{R} is the 3 A -dimensional vector $\mathbf{r}_1, \mathbf{r}_2, \dots, \mathbf{r}_A$ denoting the positions of all the nucleons in the nucleus,

$$G(\mathbf{r}) = G(r) = \frac{m^2}{2\pi^2} \frac{\Delta\tau}{(r^2 + \Delta\tau^2)} K_2[m(r^2 + \Delta\tau^2)^{1/2}], \quad (3.4)$$

and $K_2(x)$ is the modified Bessel function of order 2. Note that in the limit $\Delta\tau \rightarrow 0$ this $G(r)$ does not become a δ function as in the nonrelativistic theory. At small $\Delta\tau$, $G(r)$ has a range of order $1/m$ due to the nonlocality inherent in the relativistic kinetic-energy operator. Using

$$\int d\mathbf{r} G(\mathbf{r}) = \exp(-m\Delta\tau), \quad (3.5)$$

the relativistic kinetic energy is found to be

$$T_R = \lim_{\Delta\tau \rightarrow 0} \frac{1}{\Delta\tau} \sum_i \int d\mathbf{R} \int d\mathbf{r}'_i [\Psi_l^\dagger(\mathbf{R}) - \Psi_l^\dagger(\mathbf{R} + \mathbf{r}'_i)] G(\mathbf{r}'_i) \Psi_r(\mathbf{R}). \quad (3.6)$$

Here $G(r)$ is singular at $r=0$ in the limit $\Delta\tau \rightarrow 0$; however, this singularity does not contribute to T_R since $[\Psi_l(\mathbf{R}) - \Psi_l(\mathbf{R} + \mathbf{r}'_i)] \rightarrow 0$ as $\mathbf{r}'_i \rightarrow 0$. The limit $\Delta\tau \rightarrow 0$ can be used to obtain

$$T_R = \frac{m^2}{2\pi^2} \sum_i \int d\mathbf{R} \int d\mathbf{r}'_i [\Psi_l^\dagger(\mathbf{R}) - \Psi_l^\dagger(\mathbf{R} + \mathbf{r}'_i)] \frac{1}{r_i'^2} K_2(mr_i') \Psi(\mathbf{R}). \quad (3.7)$$

It is useful to subtract the gradient and quadratic terms in the expansion of Ψ_l^\dagger about $\mathbf{r}'_i=0$. The former give zero contribution, and the quadratic terms give the nonrelativistic kinetic energy, so that

$$T_R - T_{\text{NR}} = \frac{m^2}{2\pi^2} \sum_i \int d\mathbf{R} \int d\mathbf{r}'_i [\Psi_l^\dagger(\mathbf{R}) + \mathbf{r}'_i \cdot \nabla_i \Psi_l^\dagger(\mathbf{R}) + \frac{1}{2} \sum_\alpha r_i'^2 \nabla_{i\alpha}^2 \Psi_l^\dagger(\mathbf{R}) - \Psi_l^\dagger(\mathbf{R} + \mathbf{r}'_i)] \frac{1}{r_i'^2} K_2(mr_i') \Psi(\mathbf{R}). \quad (3.8)$$

This expression is very useful because it directly computes the small difference between the relativistic and nonrelativistic kinetic energies.

In the variational MC calculations [3,6] the Metropolis algorithm is used to generate many thousands of configurations \mathbf{R}_I , $I=1, N_c$ labels the configurations, distributed with the probability $|\Psi_l^\dagger(\mathbf{R}) \Psi_r(\mathbf{R})|$. The integral over \mathbf{r}'_i is evaluated for each configuration. The radial in-

tegral over \mathbf{r}'_i is estimated by sampling \mathbf{r}'_i with probability proportional to $r_i'^4 K_2(mr_i')$. The $r_i'^4$ factor in this probability comes from observing that the leading contribution from the terms inside the square brackets in Eq. (3.8) is of order $r_i'^4$; the $r_i'^{-2}$ factor in $G(\mathbf{r}'_i)$ is canceled by the $r_i'^2$ in $d\mathbf{r}'_i$. The integration over the directions of \mathbf{r}'_i is carried out by randomly choosing three orthogonal directions. The six points along the positive and negative sides of

these directions are summed together. In this scheme all terms of first, second, and third order in \mathbf{p}_i cancel exactly. These terms do not contribute to the difference between the relativistic and nonrelativistic kinetic energies, and canceling them exactly reduces the variance of the MC sampling.

The variational wave functions used in the present calculation are of the type reported in Ref. [6]. The pair correlation F has six terms belonging to the operators $O_{ij}^p=1,6$ given in Eqs. (2.2) and (2.3). They are obtained from the solutions of the relativistic two-body equations

$$[2(p^2 + m^2)^{1/2} - 2m + \bar{v}(r) + \lambda(r)]F(r) = 0 \quad (3.9)$$

in the 1S_0 , 3S_1 - 3D_1 , 1P_1 , and 3P_2 - 3F_2 states. The $\lambda(r)$ are used to vary the $F(r)$. The propagator $G(\mathbf{r})$ is also used to solve the two-body equations in coordinate space. We write them as integro-differential equations in which the

$$\begin{aligned} & -\frac{1}{m}f''(r) + \left[\bar{v}(r) + \lambda(r) + \frac{1}{m} \frac{l(l+1)}{r^2} \right] f \\ & = \frac{2m^2}{\pi} \left\{ \int r' dr' F(r') \int_{|r-r'|}^{r+r'} x dx P_l \left[\frac{r'^2 + r^2 - x^2}{2rr'} \right] \frac{1}{x^2} K_2(mx) - \int r' dr' F(r) \int_{|r-r'|}^{r+r'} x dx \frac{1}{x^2} K_2(mx) \right. \\ & \quad \left. - \int r' dr' \left[\frac{f''(r)}{r} - \frac{l(l+1)}{r^2} F(r) \right] \frac{1}{6} \int_{|r-r'|}^{r+r'} x dx \frac{1}{x^2} K_2(mx) \right\}, \end{aligned} \quad (3.10)$$

where $f = rF$. The three terms on the right-hand side are, respectively, from $2(p^2 + m^2)^{1/2}F$, $-2mF$, and $-p^2F/m$. Equation (3.10) is solved iteratively using the solution of the last iteration to calculate the right-hand side. This method is useful when the relativistic effects in F are small, and we have verified that the coordinate- and momentum-space solutions are identical for the deuteron. It is convenient to tabulate $\int x^n K_2(mx) dx$ for the required values of n at the beginning of the calculation.

The results obtained with the H_{SR} are compared with those of NR calculations with the Argonne $v_{14,\text{NR}}$ in Tables IV and V, respectively, for ${}^3\text{H}$ and ${}^4\text{He}$. These tables also show the results obtained by including the Urbana VII three-nucleon interaction in both H_{NR} and H_{SR} . The differences between the results obtained with H_{SR} and H_{NR} are very small. Without the V_{ijk} , the E_v obtained with H_{SR} is above the $E_v(H_{\text{NR}})$ by 0.11(3) and

TABLE V. Alpha-particle results in MeV.

	\bar{v}_{14}	$v_{14,\text{NR}}$	$\bar{v}_{14} + V_{ijk}$	$v_{14,\text{NR}} + V_{ijk}$
T_{NR}	95.1(1.1)	88.5(9)	112.6(6)	105.2(7)
$T_R - T_{\text{NR}}$	-6.16(2)		-7.58(10)	
$\langle v \rangle$	-112.3(1.0)	-112.4(1.0)	-127.4(5)	-128.5(7)
$\langle V \rangle$			-5.89(10)	-5.43(15)
E_{Coul}	0.71(1)	0.70(1)	0.74(1)	0.75(1)
E_v	-22.68(7)	-23.16(7)	-27.64(10)	-27.98(7)
$\% S = \frac{3}{2}$	14.2(1)	13.7(1)	17.7(1)	16.6(1)
R_{rms} (fm)	1.59(1)	1.61(1)	1.47(1)	1.47(1)

TABLE IV. Triton results in MeV.

	\bar{v}_{14}	$v_{14,\text{NR}}$	$\bar{v}_{14} + V_{ijk}$	$v_{14,\text{NR}} + V_{ijk}$
T_{NR}	46.8(2)	43.6(4)	51.7(2)	48.7(2)
$T_R - T_{\text{NR}}$	-2.62(2)		-2.96(2)	
$\langle v \rangle$	51.4(2)	51.0(2)	-55.9(2)	-56.0(2)
$\langle V \rangle$			-1.21(2)	-1.12(2)
E_v	-7.27(2)	-7.38(2)	-8.41(2)	-8.42(2)
$\% S = \frac{3}{2}$	8.76(2)	8.32(3)	9.94(2)	9.37(2)
R_{rms} (fm)	1.78(1)	1.79(1)	1.69(1)	1.69(1)

integral term corresponds to the difference between the relativistic and nonrelativistic kinetic energies. The integrals can be reduced to a one-dimensional form depending only on $G(r)$ and the angular momentum l . For example, the radial wave equation in $S=0$ states with $J=l$ is obtained as

0.48(10) MeV for ${}^3\text{H}$ and ${}^4\text{He}$. Here $\langle v \rangle$ changes by less than 1% and T_R in the SR model is close to T_{NR} in the NR model. The $L=2$ D -state percentage is larger in the SR model by $\sim 4\%$ of its value presumably because it is easier to bend relativistic wave functions. On including V_{ijk} , the E_v obtained with the SR model is higher by 0.01(4) and 0.31(20) MeV than the $E_v(H_{\text{NR}})$ in ${}^3\text{H}$ and ${}^4\text{He}$, respectively.

There is little difference between the nuclear radii ob-

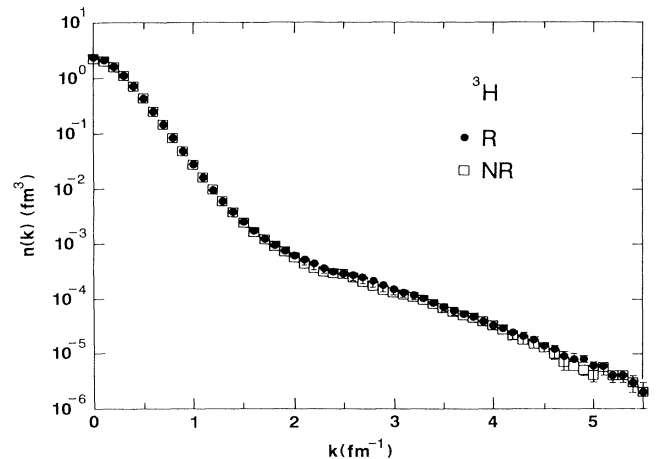


FIG. 20. Momentum distribution of the nucleons in ${}^3\text{H}$. The solid circles and open squares show results obtained with the semirelativistic and nonrelativistic calculations.

tained with the SR and NR models; the values listed in Table IV are for point nucleon rms radii. The differences between the momentum distribution $n(k)$ of nucleons are also small. The $n(k)$ in ${}^3\text{H}$ are compared in Fig. 20; the SR $n(k)$ is a bit larger than the NR $n(k)$ at $k > 2 \text{ fm}^{-1}$.

The variational wave functions used here are not the best available. In calculations using H_{NR} , Wiringa [3] has obtained $\sim 3\%$ improvements in E_0 by adding to F_{ij} spin-orbit terms and by including the three-body correlations induced by the V_{ijk} . Wiringa's results are only 3–4% above the true NR E_0 obtained with the Faddeev [8] and Green's function Monte Carlo [6] methods. However, it is unlikely that these improvements will significantly influence the comparisons between the NR and SR models presented here.

IV. $\delta v_{ij}(\mathbf{P}_{ij})$ CONTRIBUTIONS

The relativistic Hamiltonian H_R [Eq. (1.10)] contains the $\delta v_{ij}(\mathbf{P}_{ij})$ interactions in addition to H_{SR} . These interactions can be expanded in powers of $P_{ij}^2/4m^2$, and since the probability of \mathbf{P}_{ij} being larger than m is very small in nuclei, it is probably sufficient to keep only the leading terms of order $P^2/4m^2$. They have been calculated by Krajcik and Foldy [17] and Friar [25] using quantum mechanics. However, the two terms in $\delta v_{ij}(\mathbf{P}_{ij})$ considered here have simple origins in classical mechanics, as discussed below in pedagogical fashion.

In classical relativistic mechanics, the energy of two particles at rest with interparticle distance \mathbf{r}_0 is given by

$$E_0 = 2m + \bar{v}(\mathbf{r}_0). \quad (4.1)$$

Consider a frame in which these two particles are moving with velocity β . In this frame the particles have momentum

$$\mathbf{p}_1 = \mathbf{p}_2 = \mathbf{P}/2, \quad (4.2)$$

energy

$$E_{\mathbf{P}} = (E_0^2 + \mathbf{P}^2)^{1/2}, \quad (4.3)$$

and

$$\beta = P/E_{\mathbf{P}}. \quad (4.4)$$

Let the distance between the particles be \mathbf{r} and their interaction potential be $v(\mathbf{P}, \mathbf{r})$ in the moving frame. We can calculate $E_{\mathbf{P}}$ in the moving frame:

$$E_{\mathbf{P}} = 2(m^2 + P^2/4)^{1/2} + v(\mathbf{P}, \mathbf{r}). \quad (4.5)$$

Equating the expressions (4.3) and (4.5) for $E_{\mathbf{P}}$, we obtain

$$v(\mathbf{P}, \mathbf{r}) = \{ [2m + \bar{v}(\mathbf{r}_0)]^2 + P^2 \}^{1/2} - (4m^2 + P^2)^{1/2}. \quad (4.6)$$

Since we are primarily interested in momenta $P < m$, the square roots can be safely expanded to obtain

$$v(\mathbf{P}, \mathbf{r}) = \bar{v}(\mathbf{r}_0) + \frac{P^2}{2} \left[\frac{1}{2m + \bar{v}(\mathbf{r}_0)} - \frac{1}{2m} \right], \quad (4.7)$$

plus terms of order P^4 and higher. Since

$$\begin{aligned} \mathbf{r}_0 - \mathbf{r} &= [1 - (1 - \beta^2)^{1/2}] \frac{\mathbf{P} \cdot \mathbf{r}_0 \mathbf{P}}{P^2} \\ &= \frac{\mathbf{P} \cdot \mathbf{r} \mathbf{P}}{2[2m + \bar{v}(\mathbf{r})]^2}, \end{aligned} \quad (4.8)$$

$$\bar{v}(\mathbf{r}_0) = \bar{v}(\mathbf{r}) + \frac{\mathbf{P} \cdot \mathbf{r} \mathbf{P} \cdot \nabla \bar{v}(\mathbf{r})}{2[2m + \bar{v}(\mathbf{r})]^2}, \quad (4.9)$$

up to terms of order P^2 ,

$$\begin{aligned} \delta v(\mathbf{P}, \mathbf{r}) &= v(\mathbf{P}, \mathbf{r}) - \bar{v}(\mathbf{r}) \\ &= -\frac{P^2}{4m[2m + \bar{v}(\mathbf{r})]} \bar{v}(\mathbf{r}) \\ &\quad + \frac{\mathbf{P} \cdot \mathbf{r} \mathbf{P} \cdot \nabla \bar{v}(\mathbf{r})}{2[2m + \bar{v}(\mathbf{r})]^2}. \end{aligned} \quad (4.10)$$

As discussed later, almost all the contribution of $\delta v(\mathbf{P}, \mathbf{r})$ in nuclei comes from the region $r > 0.7 \text{ fm}$ in which $\bar{v}(\mathbf{r})$ is $\lesssim 5\%$ of $2m$. Hence it is appropriate to neglect the $\bar{v}(\mathbf{r})$'s in the denominator to obtain

$$\delta v(\mathbf{P}, \mathbf{r}) = -\frac{P^2}{8m^2} \bar{v}(\mathbf{r}) + \frac{1}{8m^2} \mathbf{P} \cdot \mathbf{r} \mathbf{P} \cdot \nabla \bar{v}(\mathbf{r}), \quad (4.11)$$

as used in this work.

The above calculation can be repeated for a many-body system having particles $1, 2, \dots, A$. Consider, for simplicity, that they are all at rest in a frame. Their energy in this frame is given by

$$E_0 = Am + \sum_{i < j \leq A} \bar{v}(\mathbf{r}_{ij,0}), \quad (4.12)$$

where $\mathbf{r}_{ij,0}$ are the interparticle distances in the $P=0$ frame. Now consider a frame in which this system has momentum \mathbf{P} ; i.e., each particle has momentum \mathbf{P}/A . Its energy in this frame is

$$E_{\mathbf{P}} = \left\{ \left[Am + \sum_{i < j \leq A} \bar{v}(\mathbf{r}_{ij,0}) \right]^2 + P^2 \right\}^{1/2}. \quad (4.13)$$

On expanding it in powers of P^2 and neglecting terms of order $(\bar{v}/m)^2$, we obtain

$$\begin{aligned} E_{\mathbf{P}} &= Am + \sum_{i < j \leq A} \bar{v}(\mathbf{r}_{ij}) + \frac{P^2}{2Am} \\ &\quad + \sum_{i < j \leq A} \left[\frac{\mathbf{P} \cdot \mathbf{r}_{ij} \mathbf{P} \cdot \nabla \bar{v}(\mathbf{r}_{ij})}{2A^2 m^2} - \frac{P^2}{2A^2 m^2} \bar{v}(\mathbf{r}_{ij}) \right], \end{aligned} \quad (4.14)$$

suggesting that H_R of a many-body system contains a sum of $\delta v_{ij}(\mathbf{P}_{ij})$ as assumed in Eq. (1.10). This property of $\delta v_{ij}(\mathbf{P}_{ij})$ is called ‘‘cluster separability’’ and has been discussed more generally by Coester [26].

The above classical calculation of $\delta v(\mathbf{P})$ is primarily for pedagogical purposes. These terms have been obtained earlier with quantum mechanics. The $\delta v(\mathbf{P})$ extracted from Eq. (5c) of Ref. [25] contains the above two terms, and it also has a spin-rotated term, which in two-body systems gives zero contribution in perturbation theory. This spin-rotation term can give contributions to

TABLE VI. Results obtained with the relativistic H_R in MeV.

	${}^3\text{H}$		${}^4\text{He}$	
	\bar{v}	$\bar{v} + V_{ijk}$	\bar{v}	$\bar{v} + V_{ijk}$
$E_v(H_{\text{SR}})$	-7.27(2)	-8.41(2)	-22.68(7)	-27.64(10)
$\left\langle \frac{P^2 \bar{v}}{8m^2} \right\rangle$	0.21(1)	0.23(2)	0.89(4)	1.17(3)
$\left\langle \frac{\mathbf{P} \cdot \mathbf{r} \mathbf{P} \cdot \nabla v}{8m^2} \right\rangle$	0.10(1)	0.10(1)	0.41(1)	0.53(1)
$E_v(H_R)$	-6.96(3)	-8.08(3)	-21.38(8)	-25.97(8)
$E_v(H_R) - E_v(H_{\text{NR}})$	0.41(4)	0.34(5)	1.78(15)	2.02(25)
$-\frac{A(A-1)}{16m^2} \langle P_{ij}^2 \rangle \langle \bar{v}_{ij} \rangle$	0.21	0.26	0.95	1.27

the binding energies via the small P -wave components in the wave functions of ${}^3\text{H}$ and ${}^4\text{He}$. It is neglected in the present work.

The contributions of the $\delta v_{ij}(\mathbf{P}_{ij}, \mathbf{r}_{ij})$ are calculated in first-order perturbation theory after the energy has been minimized with H_{SR} . We calculate $\mathbf{P}_{ij}|\Psi_r\rangle$, $P_{ij}^2|\Psi_r\rangle$, and $\langle \Psi_l | \mathbf{P}_{ij}$ numerically by moving particles. The expectation values of $P_{ij}^2 \bar{v}_{ij}$ and $\mathbf{P}_{ij} \cdot \mathbf{r}_{ij} \mathbf{P}_{ij} \cdot \nabla \bar{v}_{ij}(\mathbf{r}_{ij})$ are easily obtained by using these, since \mathbf{P}_{ij} commutes with \bar{v}_{ij} , \mathbf{r}_{ij} , and $\nabla \bar{v}_{ij}(\mathbf{r}_{ij})$. The results for ${}^3\text{H}$ and ${}^4\text{He}$ are given in Table VI. It is obvious from these results that these $\delta v_{ij}(\mathbf{P}_{ij}, \mathbf{r}_{ij})$ terms give most of the difference between the energies obtained with the relativistic and nonrelativistic Hamiltonians.

In order to study the dependence of the δv_{ij} contribution on r_{ij} , we calculated the expectation values of the interactions

$$\sum_{i < j} -\frac{1}{8m^2} P_{ij}^2 \bar{v}_{ij}(\mathbf{r}_{ij}) \theta(r_m - r_{ij}) \quad (4.15)$$

and

$$\sum_{i < j} \frac{1}{8m^2} \mathbf{P} \cdot \mathbf{r}_{ij} \theta(r_m - r_{ij}) \mathbf{P} \cdot \nabla \bar{v}_{ij}(\mathbf{r}_{ij}), \quad (4.16)$$

cutoff at $r_{ij} = r_m$. These expectation values for $r_m = 0.5, 0.7, 1.0,$ and 2.0 fm are shown in Fig. 21. They indicate that most of the δv_{ij} contribution comes from the $r_{ij} \sim 1-2$ fm region in which $\bar{v}_{ij} \ll m$, and hence it is reasonable to neglect the \bar{v}_{ij} in the denominators ($2m + \bar{v}$) in Eq. (4.10).

The average value $\langle \bar{v}_{ij} \rangle$ is just $\langle \bar{v} \rangle / \frac{1}{2} A(A-1)$ since there are $A(A-1)/2$ pairs. The average value

$$\begin{aligned} \langle P_{ij}^2 \rangle &= \langle p_i^2 \rangle + \langle p_j^2 \rangle + 2\langle \mathbf{p}_i \cdot \mathbf{p}_j \rangle \\ &= \frac{4m}{A} T_{\text{NR}} + 2\langle \mathbf{p}_i \cdot \mathbf{p}_j \rangle. \end{aligned} \quad (4.17)$$

Since the total momentum of the nucleus is zero,

$$\left\langle \left[\sum_i \mathbf{p}_i \right]^2 \right\rangle = 0, \quad (4.18)$$

therefore

$$2\langle \mathbf{p}_i \cdot \mathbf{p}_j \rangle = -\frac{2}{A-1} \langle p_i^2 \rangle = -\frac{4m}{A(A-1)} T_{\text{NR}}. \quad (4.19)$$

From Eqs. (4.17) and (4.19), we obtain:

$$\langle P_{ij}^2 \rangle = \frac{4m}{A} \left[\frac{A-2}{A-1} \right] T_{\text{NR}}. \quad (4.20)$$

The values of

$$-\frac{A(A-1)}{16m^2} \langle P_{ij}^2 \rangle \langle \bar{v}_{ij} \rangle = -\frac{1}{2m} \frac{1}{A} \left[\frac{A-2}{A-1} \right] T_{\text{NR}} \langle \bar{v} \rangle \quad (4.21)$$

are listed in Table VI; they are fairly close to the calculated expectation values of the $-P^2 \bar{v} / 8m^2$ term. Thus it appears that \mathbf{P}_{ij} and $\bar{v}_{ij}(\mathbf{r}_{ij})$ are not strongly correlated, and Eq. (4.21) can be used to estimate the largest relativistic effect in the present work.

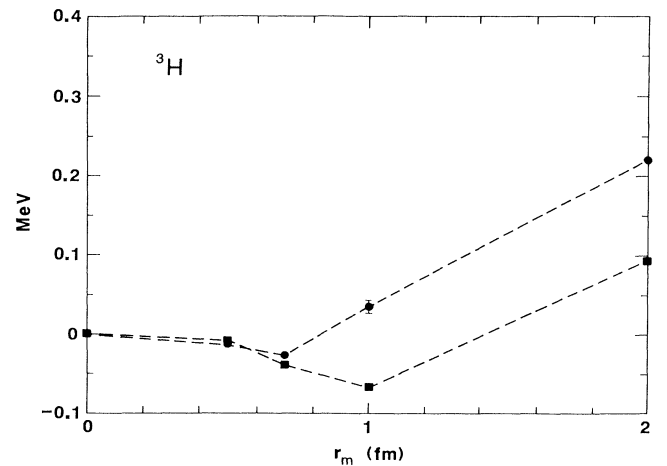


FIG. 21. Contributions of the cutoff interaction given by Eq. (4.15) (circles) and (4.16) (squares) as a function of the radius r_m . The dashed lines joining data points are purely for convenience.

V. CONCLUSIONS

The estimated relativistic effect in the binding energy of ${}^3\text{H}$, i.e., the difference between the energies obtained with H_R and H_{NR} , is 0.41 MeV without V_{ijk} . This effect has been estimated to be ~ 0.2 MeV by Glöckle, Lee, and Coester (GLC) [19] in a conceptually similar calculation also without V_{ijk} . There are two main differences between the present and GLC calculations. GLC use a modified Malfliet-Tjon interaction in place of the realistic \bar{v} used here, and they do not expand $\delta v_{ij}(\mathbf{P}_{ij})$ in powers of $P_{ij}^2/4m^2$; however, the terms of order $P_{ij}^2/4m^2$ in their $\delta v_{ij}(\mathbf{P}_{ij})$ are identical to those used here. In retrospect, it appears that the smaller relativistic effect obtained by GLC is due to their use of the simple Malfliet-Tjon interaction which does not contain the pion-exchange tensor force. The T_{NR} and $\langle v \rangle$ obtained with this potential are, respectively, 29 and -36 MeV instead of the 47 and -51 MeV (Table IV) given by the realistic \bar{v} . The leading relativistic correction is proportional to $T_{NR}\langle v \rangle$, and hence the GLC estimate of it is approximately half of ours.

The approximation (4.21) can be used to estimate the contribution of the $-\mathbf{P}^2\bar{v}/8m^2$ terms to the binding energy of nuclear matter. At the empirical equilibrium density $\rho_0=0.16\text{ fm}^{-3}$, the values of T_{NR}/A and $\langle v \rangle/A$ are, respectively, 45 and -56 MeV with the Argonne $v_{14,NR}+V_{ijk}$ [5]. Using these, we expect the $-\mathbf{P}^2\bar{v}/8m^2$ terms to give ~ 1.34 MeV per nucleon. The total relativistic correction in ${}^3\text{H}$ and ${}^4\text{He}$ is approximately twice the contribution of the $-\mathbf{P}^2\bar{v}/8m^2$ terms, and thus it could be ~ 2.5 MeV per nucleon in the present approach. It is interesting to note that the difference between the lowest-order Dirac-Brueckner and NR-Brueckner calculations [14] of the energy of nuclear matter is also ~ 2 MeV/nucleon at ρ_0 . However, the relations between the present and Dirac-Brueckner approach are not yet understood.

The model VII of V_{ijk} contains the Fujita-Miyazawa two-pion exchange $V_{ijk}^{2\pi}$ and a phenomenological repulsive term V_{ijk}^R . The strengths of these two terms are obtained by fitting the binding energies of ${}^3\text{H}$ and ${}^4\text{He}$ and the equilibrium density of nuclear matter using NRQM. Here $\langle V^R \rangle$ is 0.62 and 3.53 MeV in calculations with H_R and 0.71 and 4.17 MeV in calculations with H_{NR} in ${}^3\text{H}$ and ${}^4\text{He}$, respectively. The relativistic effects in the binding energies of ${}^3\text{H}$ and ${}^4\text{He}$ are almost half of $\langle V^R \rangle$. Thus we would presumably need a weaker V_{ijk}^R to fit the ob-

served properties of nuclei with the relativistic Hamiltonian. However, we must be able to study the energies and radii of a few heavy nuclei with the H_R in order to obtain realistic models of \bar{V}_{ijk} . In heavy nuclei the contribution of the spin-rotation term in $\delta v(\mathbf{P})$ also needs to be evaluated.

During the course of this work, Rupp and Tjon [27] reported results of ${}^3\text{H}$ calculations using Bethe-Salpeter-Faddeev (BSF) equations. Their estimate of the correction of the ${}^3\text{H}$ binding energy, due to relativistic effects, is ~ -0.3 MeV, quite different from the $+0.3$ MeV found in the present work. There are at least two major differences between the BSF and present approach. The free-particle propagator used in the BSF equation is $1/[k_0^2-\mathbf{k}\cdot\mathbf{k}-m^2+i\epsilon]$; it allows propagation with both positive and negative energies. In contrast, the free-particle propagator of the present relativistic Hamiltonian, $1/[E+m-(m^2+\mathbf{k}\cdot\mathbf{k})^{1/2}+i\epsilon]$, has propagation with only positive energies since the eigenvalues of $(m^2+\mathbf{k}\cdot\mathbf{k})^{1/2}$ are positive by definition. Second, the methods used to make the interaction covariant are also different. Rupp and Tjon use separable approximations to realistic interactions. In the nonrelativistic calculations, these are functions of the relative three-momentum square $\mathbf{p}\cdot\mathbf{p}$, while in the relativistic calculations they are assumed to be functions of the four-momentum squared, i.e., $p_0^2-\mathbf{p}\cdot\mathbf{p}$. Which of these differences is primarily responsible for the different final results obtained in Ref. [27] and the present work is also not known. Nevertheless, these differences clearly indicate that relativistic corrections to nuclear binding energies may depend strongly on the method used to generalize the NR Hamiltonian for use in relativistic calculations. The present approach may prove to be useful if the compositeness of nucleons plays an important role in suppressing the antinucleon degrees of freedom and if classical relativistic corrections dominate.

ACKNOWLEDGMENTS

The authors would like to thank Dr. Fritz Coester and Dr. Jim Friar for valuable discussions. The work of J.C. is supported by the U.S. Department of Energy, that of V.R.P. by the U.S. National Science Foundation under Grant No. PHY 89-21025, and that of R.S. by the U.S. Department of Energy, Nuclear Physics Division, under Contract No. W-31-109-ENG-38, and the Italian Istituto Nazionale di Fisica Nucleare.

-
- [1] H. Kümmel, K. H. Lührmann, and J. G. Zabolitsky, Phys. Rep. C **36**, 1 (1978).
 [2] B. D. Day and R. B. Wiringa, Phys. Rev. C **32**, 1057 (1985).
 [3] R. B. Wiringa, Phys. Rev. C **43**, 1585 (1991).
 [4] S. C. Pieper, R. B. Wiringa, and V. R. Pandharipande, Phys. Rev. Lett. **64**, 364 (1990).
 [5] R. B. Wiringa, V. Fiks, and A. Fabrocini, Phys. Rev. C **38**, 1010 (1988).

- [6] J. Carlson, Phys. Rev. C **38**, 1879 (1988).
 [7] J. Carlson, Nucl. Phys. **A508**, 141c (1990).
 [8] C. R. Chen, G. L. Payne, J. L. Friar, and B. F. Gibson, Phys. Rev. C **33**, 1740 (1986).
 [9] W. Glöckle, H. Witala, and Th. Cornelius, Nucl. Phys. **A508**, 115c (1990).
 [10] T. Sasakawa and S. Ishikawa, Few-Body Syst. **1**, 3 (1986).
 [11] B. D. Serot and J. D. Walecka, Adv. Nucl. Phys. **16**, 1 (1986).

- [12] C. J. Horowitz and B. D. Serot, Nucl. Phys. **A368**, 501 (1981).
- [13] L. S. Celenza, Shun-fu Gao, and C. M. Shakin, Phys. Rev. C **41**, 1768 (1990).
- [14] R. Brockmann and R. Machleidt, Phys. Rev. C **42**, 1965 (1990).
- [15] A. Amorim and J. A. Tjon, Phys. Rev. Lett. **68**, 772 (1992).
- [16] B. Bakamjian and L. H. Thomas, Phys. Rev. **92**, 1300 (1952).
- [17] R. A. Krajcik and L. L. Foldy, Phys. Rev. D **10**, 1777 (1974).
- [18] F. Coester, S. C. Pieper, and F. J. D. Serduke, Phys. Rev. C **11**, 1 (1975).
- [19] W. Glöckle, T.-S. H. Lee, and F. Coester, Phys. Rev. C **33**, 709 (1986).
- [20] I. E. Lagaris and V. R. Pandharipande, Nucl. Phys. **A359**, 331 (1981).
- [21] R. B. Wiringa, R. A. Smith, and T. L. Ainsworth, Phys. Rev. C **19**, 1207 (1984).
- [22] M. Lacombe *et al.*, Phys. Rev. C **21**, 861 (1980).
- [23] A. M. Green and P. Haapakoski, Nucl. Phys. **A221**, 429 (1974).
- [24] W. Glöckle, *The Quantum Mechanical Few-Body Problem* (Springer-Verlag, Berlin, 1983).
- [25] J. L. Friar, Phys. Rev. C **12**, 695 (1975).
- [26] F. Coester, Helv. Phys. Acta **38**, 7 (1965).
- [27] G. Rupp and J. A. Tjon, Phys. Rev. C **45**, 2133 (1992).